COMPUTATIONAL MECHANICS
WCCM VI in conjunction with APCOM'04, *Sept. 5-10, 2004, Beijing, China*

A Variational Multiscale Stabilized Finite Element Method for Stochastic Advection-Diffusion and Stochastic Incompressible Flow

N. Zabaras[1*], V. A. Badri Narayanan[1]

[1*] *Materials Process Design and Control Laboratory, Sibley School of Mechanical and Aerospace Engineering, Cornell University, 188 Frank H.T. Rhodes Hall, Ithaca, NY, 14853-3801, USA.*
e-mail: zabaras@cornell.edu, bnv2@cornell.edu

Abstract An extension of the deterministic variational multiscale (VMS) approach with algebraic subgrid scale (SGS) modeling is considered for developing stabilized finite element formulations for the linear stochastic scalar advection-diffusion equation and the incompressible stochastic Navier-Stokes equations. The stabilized formulations are numerically implemented using the spectral stochastic formulation of the finite element method (SSFEM). Generalized polynomial chaos and Karhunen-Loève expansion techniques are used for representation of uncertain quantities. A parallel finite element implementation using cluster specific implementation of BLAS I and BLAS II and a preconditioned parallel GMRES solver with restart capability were developed for the parallel solution of the stochastic partial differential equations. The proposed stabilized method is demonstrated by examining flow past a cylinder with uncertainties in the inflow boundary conditions.

Key words: Variational multiscale, stabilized FEM, Polynomial chaos, Karhunen-Loève, Spectral stochastic FEM, parallel GMRES, subgrid scale modeling, stochastic PDEs

INTRODUCTION

Extensive research in stabilized finite element techniques has been devoted towards deterministic fluid flow and transport systems. These techniques involve assumptions of ideal input (precise inlet boundary conditions, initial conditions, material properties and computational domain). In practice, this is hardly the case as the input is always polluted with uncertainties [1, 2]. Through the last decade, the stabilization approaches have advanced from the basic Streamline-Upwind/Petrov-Galerkin SUPG to the most recent variational multiscale VMS approach. It has been shown that the stabilization schemes arising from the VMS approach encompasses other stabilization approaches and hence it has been considered as a computational paradigm for stabilized finite element techniques [3]-[6].
With the development of the spectral stochastic finite element method Ghanem and Spanos [7] wherein stochastic system response (e.g. stochastic velocity field) is represented as a sum of projections on an appropriate Hilbert space of random variables, extensive advances have been made in the computational investigation of stochastic flow systems viz. finite-difference methods [8, 9] and spectral techniques [10, 11]. However, none of these techniques fall utilize the inherent advantages of finite element methods owing to the lack of a consistent stabilization framework. This paper attempts at extending the VMS approach to address the above issue in the context of convection dominant systems.
The paper is organized as follows. We begin with an introduction to the spectral stochastic framework. This is followed by the definition of a stochastic convection-diffusion and stochastic incompressible Navier-Stokes equations. The variational multiscale method is then introduced and the stabilized finite element formulations are derived for the above equations. An important flow problem is then

considered to demonstrate the proposed stabilization approach. Conclusions and inferences based on the numerical results are drawn.

MATHEMATICAL FRAMEWORK FOR REPRESENTATION OF UNCERTAINTY

In order to develop a rigorous mathematical framework for representation of uncertainty, we begin with the definition of a probability space $(\Omega, \mathcal{F}, \mathcal{P})$, where, Ω is the sample space or the collection of all possible basic outcomes of a mathematical experiment, $\mathcal{F}$ is the minimal sigma-algebra of the subsets of sample space and $\mathcal{P}$ is the probability measure defined on $\mathcal{F}$. For notational convenience, the probability space will be referred to by the symbol Ω. Under this framework, a real-valued random variable is defined as a function that maps the probability space to the real line or a subset of it. In other words, if Z is a real random variable, then $Z(\omega) : \Omega \mapsto \mathbb{R}$, where ω refers to the probability space.
We also define the function space $L_{\mathrm{q}}(\Omega) : q \geq 1$ is defined as the set of all random variables $Z(\omega)$ that have the following property

$$\mathbb{E}[|Z|^q] := \int_{\Omega} |Z(\omega)|^q \mathrm{d}\mathcal{P}(\omega) := \int_{\mathbb{R}} |z|^q \mathrm{d}F_{\mathrm{Z}}(x) < \infty \tag{1}$$

where, $\mathbb{E}[\bullet]$ is the mathematical expectation operator, $\mathrm{d}F_{\mathrm{Z}}(z)$ is a probability density measure that is related to $\mathcal{P}(\omega)$ through the relation $F_{\mathrm{Z}}(\mathbb{B}) = \mathcal{P}(Z^{-1}(\mathbb{B}))$, where $\mathbb{B}$ is a subset of the real line. By definition $F(x)$ is a non-decreasing function. We will assume that $F_{\mathrm{Z}}(z)$ is differentiable everywhere and hence the probability density function PDF of $Z(\omega)$ exists and is defined as $f_{\mathrm{Z}}(z) = \mathrm{d}F_{\mathrm{Z}}(z)/\mathrm{d}z$. Such a random variable with a well-defined PDF is called a continuous random variable and is a good assumption for modeling many physical quantities like transport coefficients, material data, etc.
Typically, inputs with known correlation structures are represented using their Karhunen-Loève expansions (KLE).

Karhunen-Loéve expansion and lower dimensional representation of stochastic processes
Let $W(\mathbf{x}, t, \omega)$ be a second order stochastic processes i.e. at each given spatial and temporal location $\mathbf{x}_1$ and t_1, the random variable corresponding to $W(\mathbf{x}_1, t_1, \omega)$ belongs to the function space $L_2(\Omega)$. The KLE of the process can be written as

$$W(\mathbf{x}, t, \omega) = \mathbb{E}[W](\mathbf{x}, t) + \sum_{\mathrm{i}=1}^{\infty} \sqrt{\lambda_{\mathrm{i}}} W_{\mathrm{i}}(\mathbf{x}, t) Z_{\mathrm{i}}(\omega) \tag{2}$$

where, λ_{i} and $W_{\mathrm{i}}(\mathbf{x}, t)$ are defined through the eigenvalue problem related to the Covariance kernel $R_{\mathrm{hh}}(\mathbf{y}_1, \mathbf{y}_2)$

$$\int_{\mathcal{D}\times\mathcal{T}} R_{\mathrm{hh}}(\mathbf{y}_1, \mathbf{y}_2) W_{\mathrm{i}}(\mathbf{y}_2) \mathrm{d}\mathbf{y}_2 = \lambda_{\mathrm{i}} W_{\mathrm{i}}(\mathbf{y}_1) \tag{3}$$

KLE is optimal in the sense that it minimizes the mean square error resulting from truncating the expansion in Eq (2) to a finite number of terms. However, construction of the KLE requires the knowledge of the covariance function. This is available only for the inputs of a physical system. As a consequence, we need to look for other kinds of representations for outputs of a continuum system e.g- flow and temperature patterns in a natural convection system.

Representation of uncertainty in the input of continuum systems
Typically, by employing KLE the inputs to a stochastic continuum system can be approximated in terms of a finite set of independent random variables $(Z_1, \ldots, Z_{\mathrm{n}})$, where the quantity n is called the dimensionality of the stochastic input or simply the KL dimension. We consider the following expansion technique for system output.

Generalized polynomial chaos expansion GPCE
Generalized polynomial chaos expansion employs hypergeometric Askey polynomials to construct L_2

convergent expansions to represent system outputs. Consider a continuum system with random inputs represented as a collection of random variables $\{Z_1(\omega), \dots, Z_{\rm n}(\omega)\}$. The output response $W(\mathbf{x}, t, \omega)$ of the system can be represented in a Generalized polynomial chaos expansion as follows

$$W(\mathbf{x}, t, \omega) = a_0(\mathbf{x}, t) I_0 + \sum_{\rm i_1=1}^{\rm N} a_{\rm i_1}(\mathbf{x}, t) I_1(Z_{\rm i_1}(\omega)) + \sum_{\rm i_1=1}^{\rm N} \sum_{\rm i_2=1}^{\rm i_1} a_{\rm i_1 i_2}(\mathbf{x}, t) I_2(Z_{\rm i_1}(\omega), Z_{\rm i_2}(\omega)) \cdots \tag{4}$$

$$:= \sum_{\rm i=0}^{\infty} W_{\rm i}(\mathbf{x}, t) \psi_{\rm i}(\omega) \tag{5}$$

where, $I_{\rm k}(Z_{\rm i_1}(\omega), \dots, Z_{\rm i_2}(\omega))$ denotes a hypergeometric polynomial from the Wiener-Askey series of orthogonal polynomials. The functions $\psi_{\rm i}(\omega)$ are one-to-one functions of $I_{\rm k}(Z_{\rm i_1}(\omega), \dots, Z_{\rm i_2}(\omega)) : k \geq 0$ and are introduced for notational convenience. We emphasize here that the convergence properties of Eq (4) are greatly enhanced by choosing an orthogonal polynomial with weighting function of the same functional form as the joint PDF of the system inputs.

DEFINITION OF LINEAR STOCHASTIC ADVECTION-DIFFUSION AND INCOMPRESSIBLE STOCHASTIC NAVIER-STOKES EQUATIONS

Consider $\mathcal{D}$ to be a closed region with piecewise smooth boundary Γ in d-dimensional Euclidean space $\mathbb{R}^{\rm d}$. The set of equations governing the transient advection and diffusion of a passive scalar field $\phi(\mathbf{x}, t, \omega)$ in a divergence-free velocity field $\mathbf{a}(\mathbf{x}, \omega)$ in a medium with diffusion coefficient $\nu(\omega)$ can be specified as

$$\partial_{\rm t}\phi + \mathbf{a}\bullet\nabla\phi - \nabla\bullet(\nu\nabla\phi) = f, \quad (\mathbf{x}, t, \omega) \in (\mathcal{D} \times \mathcal{T} \times \Omega) \tag{6}$$

The incompressible Navier-Stokes set of equations describing the flow of a fluid with random viscosity $\nu(\omega)$ can be described as follows

$$\frac{\partial \boldsymbol{v}}{\partial t} + \boldsymbol{v}\bullet\nabla\boldsymbol{v} = \nabla\bullet\boldsymbol{\sigma} + \mathbf{f} \tag{7}$$

where the constitutive relations describing the stress tensor are

$$\boldsymbol{\sigma} = -p\boldsymbol{I} + 2\nu(\omega)\boldsymbol{\epsilon}(\boldsymbol{v}) \qquad \boldsymbol{\epsilon}(\boldsymbol{v}) = [\nabla\boldsymbol{v} + (\nabla\boldsymbol{v})^T]/2 \tag{8}$$

In the above equations, Ω denotes the probability space, $\mathcal{T}$ is a closed time interval, $\boldsymbol{I}$ is the second-order unit tensor, p is the stochastic pressure and $\boldsymbol{v}$ is the stochastic velocity. The quantities f and $\mathbf{f}$ are stochastic scalar and vector source terms. Further, the incompressibility constraint takes the form

$$\nabla\bullet\boldsymbol{v} = 0, \quad (\mathbf{x}, t, \omega) \in (\mathcal{D} \times \mathcal{T} \times \Omega) \tag{9}$$

In order to complete the description of these problems, we consider the following Dirichlet boundary conditions and initial conditions:

$$\boldsymbol{v}(\mathbf{x}, t, \omega) = \boldsymbol{v}_{\rm g}(\mathbf{x}, t, \omega), \quad (\mathbf{x}, t, \omega) \in (\Gamma \times \mathcal{T} \times \Omega) \tag{10}$$

$$\boldsymbol{v}(\mathbf{x}, 0, \omega) = \boldsymbol{v}_0(\mathbf{x}, \omega), \quad (\mathbf{x}, t, \omega) \in (\mathcal{D} \times \{0\} \times \Omega) \tag{11}$$

$$\phi(\mathbf{x}, t, \omega) = \phi_{\rm g}(\mathbf{x}, t, \omega), \quad (\mathbf{x}, t, \omega) \in (\Gamma \times \mathcal{T} \times \Omega) \tag{12}$$

$$\phi(\mathbf{x}, 0, \omega) = \phi_0(\mathbf{x}, \omega), \quad (\mathbf{x}, t, \omega) \in (\mathcal{D} \times \{0\} \times \Omega) \tag{13}$$

We emphasize here that the choice of boundary condition is to facilitate the ensuing discussion. More complicated boundary conditions can be handled easily.

VARIATIONAL MULTISCALE STABILIZED FORMULATION

We define the function spaces $U, V, \mathbf{U}, \mathbf{V}$ and X as follows

$$
\begin{aligned}
U &= \{u : u(\mathbf{x}, t, \omega) \in H^1(\mathcal{D}) \times L_2(\Omega), \quad u = \phi_{\mathrm{g}}, \quad \forall\, \mathbf{x} \in \Gamma\} && (14)\\
V &= \{u : u(\mathbf{x}, t, \omega) \in H^1(\mathcal{D}) \times L_2(\Omega), \quad u = 0, \quad \forall\, \mathbf{x} \in \Gamma\} && (15)\\
\mathbf{U} &= \{\boldsymbol{v} : \boldsymbol{v}(\mathbf{x}, t, \omega) \in H^1(\mathcal{D}) \times L_2(\Omega), \quad \boldsymbol{v} = \boldsymbol{v}_{\mathrm{g}}, \quad \forall\, \mathbf{x} \in \Gamma\} && (16)\\
\mathbf{V} &= \{\boldsymbol{v} : \boldsymbol{v}(\mathbf{x}, t, \omega) \in H^1(\mathcal{D}) \times L_2(\Omega), \quad \boldsymbol{v} = 0, \quad \forall\, \mathbf{x} \in \Gamma\} && (17)\\
X &= \{u : u(\mathbf{x}, t, \omega) \in L_2(\mathcal{D}) \times L_2(\Omega)\} && (18)
\end{aligned}
$$

The weak form for the equations (6), (7) and (9) can be written as follows:
Find $\phi \in U$ such that for all $w \in V$ and $t \in \mathcal{T}$, the following hold

$$(\partial_{\mathrm{t}}\phi, w) + (\mathbf{a}\bullet \nabla\phi, w) + (\nu\nabla\phi, \nabla w) = (f, w) \tag{19}$$

Find $\boldsymbol{v} \in \mathbf{U}$ and $p \in X$ such that for all $\boldsymbol{w} \in \mathbf{V}$, $q \in X$ and $t \in \mathcal{T}$, the following hold

$$(\partial_{\mathrm{t}}\boldsymbol{v}, \boldsymbol{w}) + (\boldsymbol{v}\bullet \nabla\boldsymbol{v}, \boldsymbol{w}) + (\nu\nabla\boldsymbol{v}, \nabla\boldsymbol{w}) - (p, \nabla\bullet \boldsymbol{w}) = (\mathbf{f}, \boldsymbol{w}) \tag{20}$$

$$(\nabla\bullet \boldsymbol{v}, q) = 0 \tag{21}$$

Under the variational multiscale hypothesis, the solution to a system of partial differential equations is considered to be a combination of two different scale components i) the resolved/large-scale component and ii) the unresolved/ small-scale/subgrid component. Typically, methods like standard Galerkin FEM can capture the large-scale solution, however, for convection dominant systems the mesh size should be of the order of viscosity and hence is computationally restrictive.
Here, we consider an overlapping sum decomposition for the solution quantities $\phi, \boldsymbol{v}$ and p as follows:

$$\phi = \bar{\phi} + \phi', \quad \boldsymbol{v} = \bar{\boldsymbol{v}} + \boldsymbol{v}', \quad p = \bar{p} + p' \tag{22}$$

where, the quantities with a bar indicate the resolved solution and the quantities with a prime (') indicate the subgrid solution. We typically desire to explicitly represent the resolved solution components using finite elements and model the effect of subgrid solutions on the resolved scales.
The above decomposition for solution quantities leads to similar decomposition for the associated function spaces and the weighting functions

$$U = \bar{U} + U', V = \bar{V} + V', \mathbf{U} = \bar{\mathbf{U}} + \mathbf{U}', \mathbf{V} = \bar{\mathbf{V}} + \mathbf{V}', X = \bar{X} + X' \tag{23}$$

Further, the subgrid solutions are assumed to be quasi-static $\partial_{\mathrm{t}}\phi' \approx \partial_{\mathrm{t}}\boldsymbol{v}' \approx 0$, the flow is assumed to be laminar so that the nonlinear advection term can be linearized using one-step Picard's linearization as $\boldsymbol{v}\bullet \nabla\boldsymbol{v} \approx \bar{\boldsymbol{v}}\bullet \nabla\bar{\boldsymbol{v}} + \bar{\boldsymbol{v}}\bullet \nabla\boldsymbol{v}'$. The weak forms given by Eqs (19, 20 and 21) can be simplified to obtain the following weak forms for the resolved scales and the subgrid scales for the linear stochastic advection-diffusion equation

$$
\begin{aligned}
(\partial_{\mathrm{t}}\bar{\phi}, \bar{w}) + (\mathbf{a}\bullet \nabla(\bar{\phi} + \phi'), \bar{w}) + (\nu\nabla(\bar{\phi} + \phi'), \nabla\bar{w}) &= (f, \bar{w}) && (24)\\
(\partial_{\mathrm{t}}\bar{\phi}, w') + (\mathbf{a}\bullet \nabla(\bar{\phi} + \phi'), w') + (\nu\nabla(\bar{\phi} + \phi'), \nabla w') &= (f, w') && (25)
\end{aligned}
$$

The following weak forms are obtained for the incompressible stochastic Navier-Stokes equations

$$
\begin{aligned}
&(\partial_{\mathrm{t}}\bar{\boldsymbol{v}}, \bar{\boldsymbol{w}}) + (\bar{\boldsymbol{v}}\bullet \nabla(\bar{\boldsymbol{v}} + \boldsymbol{v}'), \bar{\boldsymbol{w}}) + (\nu\nabla(\bar{\boldsymbol{v}} + \boldsymbol{v}'), \nabla\bar{\boldsymbol{w}}) - (\bar{p} + p', \nabla\bullet \bar{\boldsymbol{w}}) = (\mathbf{f}, \bar{\boldsymbol{w}}) && (26)\\
&(\partial_{\mathrm{t}}\bar{\boldsymbol{v}}, \boldsymbol{w}') + (\bar{\boldsymbol{v}}\bullet \nabla(\bar{\boldsymbol{v}} + \boldsymbol{v}'), \boldsymbol{w}') + (\nu\nabla(\bar{\boldsymbol{v}} + \boldsymbol{v}'), \nabla\boldsymbol{w}') - (\bar{p} + p', \nabla\bullet \boldsymbol{w}') = (\mathbf{f}, \boldsymbol{w}') && (27)\\
&(\nabla\bullet (\bar{\boldsymbol{v}} + \boldsymbol{v}'), \bar{q}) = 0 && (28)\\
&(\nabla\bullet (\bar{\boldsymbol{v}} + \boldsymbol{v}'), q') = 0 && (29)
\end{aligned}
$$

Assuming a finite element discretization of the spatial domain as $\cup_{\mathrm{e}=0}^{\mathrm{Nel}}\mathcal{D}^{(\mathrm{e})}$, Eq (25) together with stronger regularity conditions can be written as

$$\mathbf{a}\bullet \nabla\phi' - \nabla\bullet (\nu\nabla\phi') = R_{\mathrm{ad}}\bar{\phi} \quad \text{on} \quad \mathcal{D}^{(\mathrm{e})}, \quad \phi' = 0, \quad \text{on} \quad \Gamma^{(\mathrm{e})} \tag{30}$$

where, $R_{\rm ad}\bar{\phi} = f - \partial_{\rm t}\bar{\phi} - \mathbf{a}\boldsymbol{\cdot}\nabla\bar{\phi} + \nabla\boldsymbol{\cdot}(\nu\nabla\bar{\phi})$ is the residual for the resolved solution. Eqs (27 and 29) together with stronger regularity conditions can be written as

$$\bar{\boldsymbol{v}}\boldsymbol{\cdot}\nabla\boldsymbol{v}' - \nabla\boldsymbol{\cdot}(\nu\nabla\boldsymbol{v}') + \nabla p' = R_{\rm m}(\bar{\boldsymbol{v}}, \bar{p}), \quad \text{on} \quad \mathcal{D}^{(\rm e)} \tag{31}$$

$$\nabla\boldsymbol{\cdot}\boldsymbol{v}' = -\nabla\boldsymbol{\cdot}\bar{\boldsymbol{v}}, \quad \text{on} \quad \mathcal{D}^{(\rm e)} \quad \boldsymbol{v}' = 0, \quad \text{on} \quad \Gamma^{(\rm e)} \tag{32}$$

where $R_{\rm m}(\bar{\boldsymbol{v}}, \bar{p}) = \mathbf{f} - \partial_{\rm t}\bar{\boldsymbol{v}} - \bar{\boldsymbol{v}}\boldsymbol{\cdot}\nabla\bar{\boldsymbol{v}} + \nabla\bar{p} + \nabla\boldsymbol{\cdot}(\nu\nabla\bar{\boldsymbol{v}})$ is the resolved scale momentum residual.
By applying fourier transform to the subgrid scale equations followed by application of Plancheral's formula and mean-value theorem, we arrive at the following models for subgrid scale solution

$$\phi' \approx \tau_{\rm ad}(\mathbf{x}, \omega)R_{\rm ad}\bar{\phi}, \quad \boldsymbol{v}' \approx \tau_{\rm m}(\mathbf{x}, \omega)R_{\rm m}(\bar{\boldsymbol{v}}, \bar{p}), \quad p' \approx \tau_{\rm c}(\mathbf{x}, \omega)\bar{p} \tag{33}$$

Explicit expressions for the intrinsic subgrid time scale parameters $\tau_{\rm ad}, \tau_{\rm m}$ and $\tau_{\rm c}$ are provided in Badri Narayanan and Zabaras [12].
Finally substituting back the subgrid models into resolved scale weak forms, we get the following stabilized formulations for linear finite elements

$$(\partial_{\rm t}\bar{\phi} + \mathbf{a}\boldsymbol{\cdot}\nabla\bar{\phi} - f, \bar{w} + \tau_{\rm ad}\mathbf{a}\boldsymbol{\cdot}\nabla\bar{w}) + (\nu\nabla\bar{\phi}, \nabla\bar{w}) = 0 \tag{34}$$

$$(\partial_{\rm t}\bar{\boldsymbol{v}} + \bar{\boldsymbol{v}}\boldsymbol{\cdot}\nabla\bar{\boldsymbol{v}} - \mathbf{f}, \bar{\boldsymbol{w}} + \tau_{\rm m}\bar{\boldsymbol{v}}\boldsymbol{\cdot}\nabla\bar{\boldsymbol{w}}) + (\nu\nabla\bar{\boldsymbol{v}}, \nabla\bar{\boldsymbol{w}}) - (\bar{p}, \nabla\boldsymbol{\cdot}\bar{\boldsymbol{w}}) - (\nabla\boldsymbol{\cdot}\boldsymbol{v}, \tau_{\rm c}\nabla\boldsymbol{\cdot}\bar{\boldsymbol{v}}) = 0 \tag{35}$$

$$(\nabla\boldsymbol{\cdot}\boldsymbol{v}, \bar{q}) + (\partial_{\rm t}\bar{\phi} + \mathbf{a}\boldsymbol{\cdot}\nabla\bar{\phi} - \nabla\boldsymbol{\cdot}(\nu\nabla\boldsymbol{v}) - \nabla\bar{p} - \mathbf{f}, \tau_{\rm m}\nabla\bar{q}) = 0 \tag{36}$$

Implementation details
The stochastic inputs viz. the advection velocity, diffusion coefficient, fluid viscosity were represented in their respective Karhunen-Loève expansions. Pseudo-spectral weighting functions were used to obtain finite-element representations for the unknowns as follows

$$\bar{\phi} = \sum_{\rm m=1}^{\rm nbf\times(P+1)} \bar{\phi}_{\rm m} w_{\rm m}(\mathbf{x}, \omega), \quad w_{\rm m}(\mathbf{x}, \omega) = N_\alpha(\mathbf{x})\psi_{\rm i}(\omega) \tag{37}$$

where, nbf denotes the number of finite element basis functions per element (spatial discretization), $\psi_{\rm i}(\omega)$ is a polynomial from the Wiener-Askey series, $N_\alpha(\mathbf{x})$ is the shape-function for the element used to discretize the spatial domain and $\rm m = (\alpha - 1)(P + 1) + i$. This type of representation allows interpretation of the nodal unknowns as a vector containing the coefficients of the GPCE of the solution. Owing to the high-computational requirement of the proposed method, cluster dependant parallel versions of BLAS I and BLAS II and a platform independent parallel preconditioned GMRES solver were developed.

NUMERICAL EXAMPLES

Flow past a circular cylinder - wake flow
The computational domain shown in Fig. 1 comprises of 2000 bilinear quadrilateral elements. The simulation was carried out for $t = 144$ s with a time stepping of 0.03 s. The inlet velocity is assumed to be a uniform random variable with a probability distribution $U[0.9, 1.1]$. The kinematic viscosity is deterministic $\nu = 0.01$. No uncertainty is considered in the initial conditions. The outflow boundary is assumed to be traction-free.
It is interesting to note that the vortex shedding is initiated by the higher-order terms in the Legendre chaos expansion of the solution (velocity and pressure). Figs. 2a and 2b show that the first-order term in LCE of pressure has already entered the periodic vortex shedding regime when the mean pressure just starts exhibiting the transition to the vortex shedding regime. It is thus very important to ensure that the higher order terms are calculated accurately. Typically, due to the relatively high uncertainty level considered (10% fluctuation about the mean value), the convergence of the solver for higher order terms is severely tested.

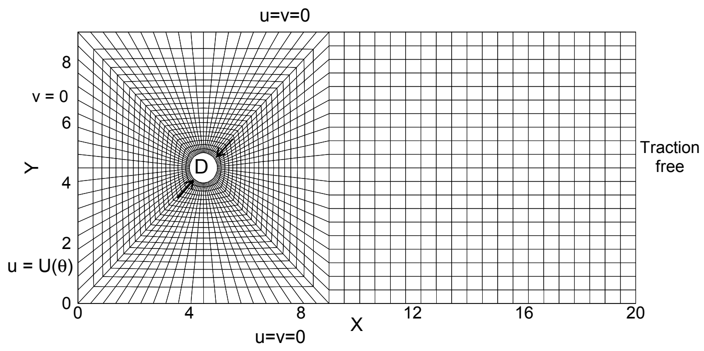

Figure 1: Problem definition and computational domain for the flow past a circular cylinder example.

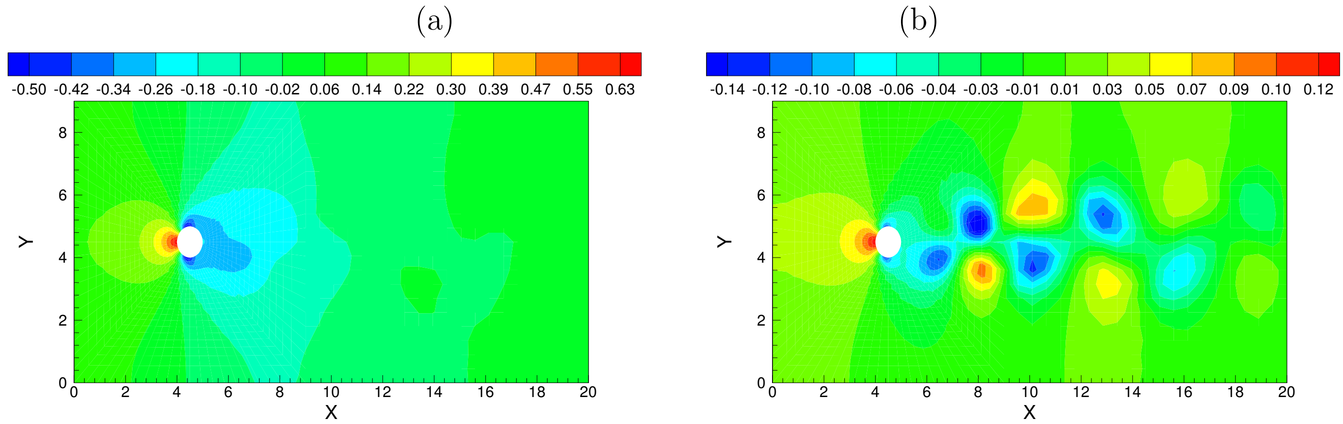

Figure 2: (a) Mean pressure and (b) First-order term in Legendre chaos expansion of pressure at $t = 79.2$ s for the flow pass a circular cylinder example.

The results at $t = 144$s are shown in Figs. 3 to 6. The mean pressure contours at $t = 144$s in Fig. 3(a) and (b) show interesting details. The stochastic mean pressure is out of phase with the deterministic pressure. This can be noticed by the shedding pattern in the wake region. Further, the near wake effects decay faster for the stochastic mean pressure. This is observed by the decay of eddies nearer to the cylinder than in the case for deterministic simulation. It can be observed that the streamline patterns for mean velocity components Fig. 4(a) and (b) also show considerable difference. Further, the deterministic streamlines indicate a stronger circulation in the near wake region than for the stochastic mean component. The comparison of velocity components for the deterministic simulation and the stochastic simulation are shown in Figs. 6(a) and (b). Again differences can be observed in magnitude and phase in both velocity components. The velocity spectrum calculated using FFT Fig. 6(c) of mean velocity is considerably broad. This is in contrast with the deterministic simulations where a sharp shedding frequency is obtained. The dominant frequency however is nearly the same as the deterministic vortex shedding frequency. A value of 0.162 was obtained for the Strouhal number based on mean velocity. This analysis of velocity spectrum is however a guideline and does not explain the essential dynamics of the uncertainty propagation. It can be observed that though the uncertainty in inlet velocity amounts to 10% fluctuation about the mean value, the pressure fluctuation after the onset of vortex shedding is about 35% of the mean value (see Figs. 5(a) and (b)).

Conclusions

We have developed a stabilized finite element framework based on the Variational multiscale method with algebraic subgrid modeling for the solution of linear stochastic scalar advection-diffusion and incompressible stochastic Navier-Stokes equations. Several numerical benchmark examples with uncertainty in boundary conditions were considered to validate the formulation and to test the numerical

(a) (b)

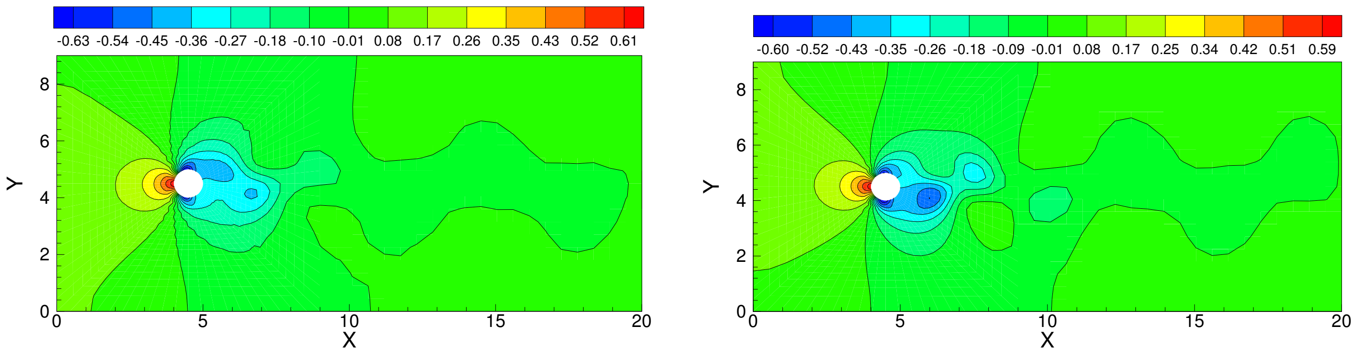

Figure 3: Mean pressure contours at $t = 144$ s for the flow pass a circular cylinder example: (a) Stochastic simulation (b) Deterministic simulation.

(a) (b)

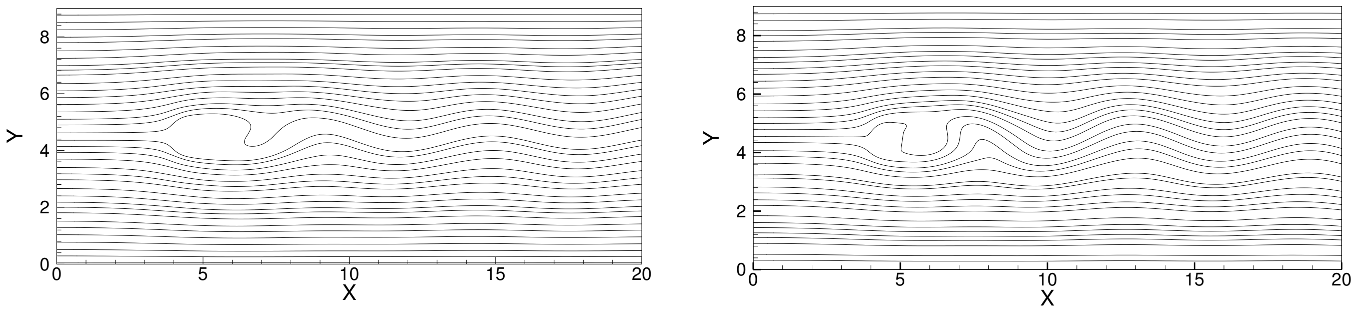

Figure 4: Mean streamline pattern $t = 144$ s for the flow pass a circular cylinder example: (a) Stochastic simulation (b) Deterministic simulation.

(a) (b)

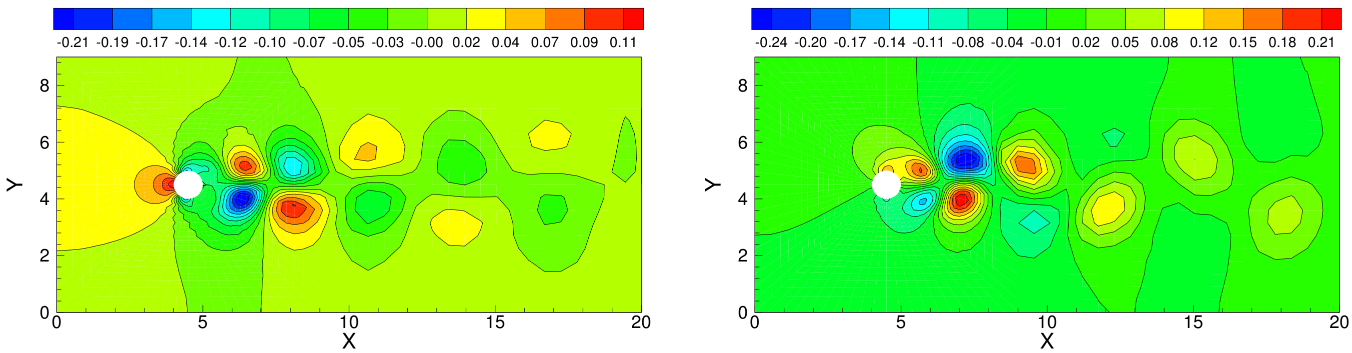

Figure 5: Higher order Legendre chaos terms for stochastic pressure solution at $t = 144$ s.

(a) (b) (c)

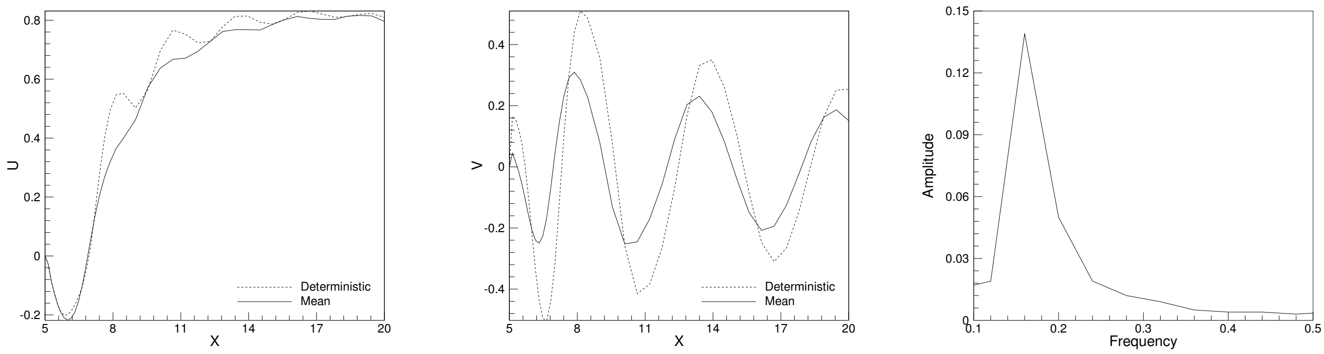

Figure 6: (a), (b) Comparison of deterministic velocity components with means of the stochastic velocity components along the centerline in the cylinder wake region. (c) Mean velocity spectrum (dc component not shown).

efficiency of the implementation
A parallel finite element implementation using cluster specific implementation of BLAS I and BLAS II and a preconditioned parallel GMRES solver with restart capability were developed for parallel solution of the coupled stochastic partial differential equations. Though the computational effort involved with the proposed method is an order of magnitude higher than that of a deterministic problem, it was still found to be two orders of magnitude faster than the Monte Carlo simulation for advection-diffusion problems. Noting the sheer computational time needed to perform a Monte Carlo on fluid flow examples that exercise was not undertaken.
The implementation however can be refined in the following areas

- Convergence rate of GMRES solver in transient problems like flow past a circular cylinder (on the onset of vortex shedding) went down drastically. New physics based preconditioning strategies need to be developed to this end.

- The solution scheme still suffers from curse of dimensionality. If the input has a steeply decaying covariance kernel, a higher dimensional Askey chaos polynomial representation is needed for the solution. This places a computational constraint on available algorithms.

- Though Askey chaos is well suited for a variety of probability distributions, if the input probability model is derived from experimental data, Askey chaos may not be sufficient to ensure exponential convergence in probability distribution. Research efforts are required in this regard.

Acknowledgements

The work presented here was funded in part by NASA, Office of Biological and Physical Sciences Research (98-HEDS-05), the Computational Mathematics program of the Air Force Office of Scientific Research (grant F49620-00-1-0373) and the Design and Integration Engineering Program of the Design Manufacture and Industrial Innovation Division of the National Science Foundation (grant DMI-0113295). This research was conducted using the resources of the Cornell Theory Center, which receives funding from Cornell University, New York State, federal agencies, and corporate partners.

References

[1] C. Mendoza and T. McAlary, *Modeling of ground-water contamination caused by organic solvent vapors*, Ground Water, 28(2), (1990), 199-206.

[2] J. Borggaard, D. Pelletier and E. Turgeon, *Parametric uncertainty analysis for thermal and fluid calculations*, Nonlinear Analysis, 47, (2001), 4533-4543.

[3] A. N. Brooks and T. J. R. Highes, *Streamline-upwind/Petro-Galerkin formulations for convective dominated flows with particular emphasis on the incompressible Navier-Stokes equations*, Comput. Meth. Appl. Mech. Engrg., 32, (1982), 199–259.

[4] T. J. R. Highes, L. P. Franca, G. M. Hulbert, *A new finite element formulation for computational fluid dynamics: VII. The Galerkin least squares method for advective-diffusive equations*, Comput. Meth. Appl. Mech. Engrg., 59, (1986), 85-99.

[5] F. Brezzi, L. P. Franca, T. J. R. Hughes and A. Russo, $b = \int g$, Comput. Meth. Appl. Mech. Engrg., 145, (1997), 329-339.

[6] T. J. R. Hughes, *Multiscale phenomena: Greens functions, the dirichlet-to-Neumann formulation, subgrid scale models, bubbles and the origin of stabilized methods*, Comput. Meth. Appl. Mech. Engrg., 127, (1995), 387-401.

[7] R. G. Ghanem and P. D. Spanos, *Stochastic finite elements: A spectral approach.*, Springer-Verlag, 1991.

[8] O. P. Le Maitre, O. M. Kino, H. N. Najm, R. Ghanem, *A stochastic projection method for fluid flow I: Basic formulation*, J. Comput. Phy., 173, (2001), 481-511.

[9] O. P. Le Maitre, M. Reagan, H. N. Najm, R. Ghanem, O. M. Knio, *A stochastic projection method for fluid flow. II: Random process*, J. Comput. Phy., 181, (2002), 9-44.

[10] D. Xiu, D. Lucor, C. -H. Su and G. E. Karniadakis, *Stochastic modeling of flow-structure interactions using generalized polynomial chaos*, J. Fluids Engrg., 125, (2001), 51-59.

[11] D. Xiu and G. E. Karniadakis, *Modeling uncertainty in flow simulations via generalized polynomial chaos*, J. Comput. Phy., 187, (2003), 137-167.

[12] V.A. Badri Narayanan and N. Zabaras, *Variational multiscale stabilized FEM formulations for transport equations: stochastic advection-diffusion and incompressible stochastic Navier-Stokes equations*, J. Comput. Phy., submitted for publication.